EUROPEAN ORGANIZATION FOR NUCLEAR RESEARCH

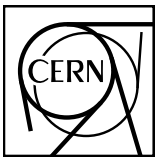

CERN-PH-EP-2015-245
September 11, 2015
rev. Dec. 14, 2015

Longitudinal double spin asymmetries in single hadron quasi-real photoproduction at high p_T

Abstract

We measured the longitudinal double spin asymmetries A_{LL} for single hadron muoproduction off protons and deuterons at photon virtuality $Q^2 < 1(\mathrm{GeV}/c)^2$ for transverse hadron momenta p_T in the range 1 GeV/c to 4 GeV/c. They were determined using COMPASS data taken with a polarised muon beam of 160 GeV/c or 200 GeV/c impinging on polarised ^{6}LiD or NH_3 targets. The experimental asymmetries are compared to next-to-leading order pQCD calculations, and are sensitive to the gluon polarisation ΔG inside the nucleon in the range of the nucleon momentum fraction carried by gluons $0.05 < x_g < 0.2$.

(Submitted to Physics Letters B)

The COMPASS Collaboration

C. Adolph[9], R. Akhunzyanov[8], M.G. Alexeev[28], G.D. Alexeev[8], A. Amoroso[28,29], V. Andrieux[22], V. Anosov[8], W. Augustyniak[31], A. Austregesilo[17], C.D.R. Azevedo[2], B. Badełek[32], F. Balestra[28,29], J. Barth[5], R. Beck[4], Y. Bedfer[22,11], J. Bernhard[14,11], K. Bicker[17,11], E. R. Bielert[11], R. Birsa[26], J. Bisplinghoff[4], M. Bodlak[19], M. Boer[22], P. Bordalo[13,a], F. Bradamante[25,26], C. Braun[9], A. Bressan[25,26], M. Büchele[10], E. Burtin[22], W.-C. Chang[23], M. Chiosso[28,29], I. Choi[30], S.-U. Chung[17,b], A. Cicuttin[27,26], M.L. Crespo[27,26], Q. Curiel[22], S. Dalla Torre[26], S.S. Dasgupta[7], S. Dasgupta[25,26], O.Yu. Denisov[29], L. Dhara[7], S.V. Donskov[21], N. Doshita[34], V. Duic[25], W. Dünnweber[c], M. Dziewiecki[33], A. Efremov[8], P.D. Eversheim[4], W. Eyrich[9], M. Faessler[c], A. Ferrero[22], M. Finger[19], M. Finger jr.[19], H. Fischer[10], C. Franco[13], N. du Fresne von Hohenesche[14], J.M. Friedrich[17], V. Frolov[8,11], E. Fuchey[22], F. Gautheron[3], O.P. Gavrichtchouk[8], S. Gerassimov[16,17], F. Giordano[30], I. Gnesi[28,29], M. Gorzellik[10], S. Grabmüller[17], A. Grasso[28,29], M. Grosse Perdekamp[30], B. Grube[17], T. Grussenmeyer[10], A. Guskov[8], F. Haas[17], D. Hahne[5], D. von Harrach[14], R. Hashimoto[34], F.H. Heinsius[10], F. Herrmann[10], F. Hinterberger[4], N. Horikawa[18,d], N. d'Hose[22], C.-Y. Hsieh[23], S. Huber[17], S. Ishimoto[34,e], A. Ivanov[8], Yu. Ivanshin[8], T. Iwata[34], R. Jahn[4], V. Jary[20], R. Joosten[4], P. Jörg[10], E. Kabuß[14], B. Ketzer[17,f], G.V. Khaustov[21], Yu.A. Khokhlov[21,g,i], Yu. Kisselev[8], F. Klein[5], K. Klimaszewski[31], J.H. Koivuniemi[3], V.N. Kolosov[21], K. Kondo[34], K. Königsmann[10], I. Konorov[16,17], V.F. Konstantinov[21], A.M. Kotzinian[28,29], O. Kouznetsov[8], M. Krämer[17], P. Kremser[10], F. Krinner[17], Z.V. Kroumchtein[8], N. Kuchinski[8], R. Kuhn[17,h], F. Kunne[22], K. Kurek[31], R.P. Kurjata[33], A.A. Lednev[21], A. Lehmann[9], M. Levillain[22], S. Levorato[26], J. Lichtenstadt[24], R. Longo[28,29], A. Maggiora[29], A. Magnon[22], N. Makins[30], N. Makke[25,26], G.K. Mallot[11], C. Marchand[22,j], B. Marianski[31], A. Martin[25,26], J. Marzec[33], J. Matoušek[19], H. Matsuda[34], T. Matsuda[15], G. Meshcheryakov[8], W. Meyer[3], T. Michigami[34], Yu.V. Mikhailov[21], Y. Miyachi[34], P. Montuenga[30], A. Nagaytsev[8], F. Nerling[14], D. Neyret[22], V.I. Nikolaenko[21], J. Nový[20,11], W.-D. Nowak[10], G. Nukazuka[34], A.S. Nunes[13], A.G. Olshevsky[8], I. Orlov[8], M. Ostrick[14], D. Panzieri[1,29], B. Parsamyan[28,29], S. Paul[17], J.-C. Peng[30], F. Pereira[2], M. Pešek[19], D.V. Peshekhonov[8], S. Platchkov[22], J. Pochodzalla[14], V.A. Polyakov[21], J. Pretz[5,k], M. Quaresma[13], C. Quintans[13], S. Ramos[13,a], C. Regali[10], G. Reicherz[3], C. Riedl[30], N.S. Rossiyskaya[8], D.I. Ryabchikov[21,i], A. Rychter[33], V.D. Samoylenko[21], A. Sandacz[31], C. Santos[26], S. Sarkar[7], I.A. Savin[8], G. Sbrizzai[25,26], P. Schiavon[25,26], K. Schmidt[10,m], H. Schmieden[5], K. Schönning[11,l], S. Schopferer[10], A. Selyunin[8], O.Yu. Shevchenko[8,*], L. Silva[13], L. Sinha[7], S. Sirtl[10], M. Slunecka[8], F. Sozzi[26], A. Srnka[6], M. Stolarski[13], M. Sulc[12], H. Suzuki[34,d], A. Szabelski[31], T. Szameitat[10,m], P. Sznajder[31], S. Takekawa[28,29], S. Tessaro[26], F. Tessarotto[26], F. Thibaud[22], F. Tosello[29], V. Tskhay[16], S. Uhl[17], J. Veloso[2], M. Virius[20], T. Weisrock[14], M. Wilfert[14], J. ter Wolbeek[10,m], K. Zaremba[33], M. Zavertyaev[16], E. Zemlyanichkina[8], M. Ziembicki[33] and A. Zink[9]

[1] University of Eastern Piedmont, 15100 Alessandria, Italy
[2] University of Aveiro, Department of Physics, 3810-193 Aveiro, Portugal
[3] Universität Bochum, Institut für Experimentalphysik, 44780 Bochum, Germany[no]
[4] Universität Bonn, Helmholtz-Institut für Strahlen- und Kernphysik, 53115 Bonn, Germany[n]
[5] Universität Bonn, Physikalisches Institut, 53115 Bonn, Germany[n]
[6] Institute of Scientific Instruments, AS CR, 61264 Brno, Czech Republic[p]
[7] Matrivani Institute of Experimental Research & Education, Calcutta-700 030, India[q]
[8] Joint Institute for Nuclear Research, 141980 Dubna, Moscow region, Russia[r]
[9] Universität Erlangen–Nürnberg, Physikalisches Institut, 91054 Erlangen, Germany[n]
[10] Universität Freiburg, Physikalisches Institut, 79104 Freiburg, Germany[no]
[11] CERN, 1211 Geneva 23, Switzerland
[12] Technical University in Liberec, 46117 Liberec, Czech Republic[p]
[13] LIP, 1000-149 Lisbon, Portugal[s]
[14] Universität Mainz, Institut für Kernphysik, 55099 Mainz, Germany[n]

[15] University of Miyazaki, Miyazaki 889-2192, Japan[t]
[16] Lebedev Physical Institute, 119991 Moscow, Russia
[17] Technische Universität München, Physik Department, 85748 Garching, Germany[nc]
[18] Nagoya University, 464 Nagoya, Japan[t]
[19] Charles University in Prague, Faculty of Mathematics and Physics, 18000 Prague, Czech Republic[p]
[20] Czech Technical University in Prague, 16636 Prague, Czech Republic[p]
[21] State Scientific Center Institute for High Energy Physics of National Research Center 'Kurchatov Institute', 142281 Protvino, Russia
[22] CEA IRFU/SPhN Saclay, 91191 Gif-sur-Yvette, France[o]
[23] Academia Sinica, Institute of Physics, Taipei, 11529 Taiwan
[24] Tel Aviv University, School of Physics and Astronomy, 69978 Tel Aviv, Israel[u]
[25] University of Trieste, Department of Physics, 34127 Trieste, Italy
[26] Trieste Section of INFN, 34127 Trieste, Italy
[27] Abdus Salam ICTP, 34151 Trieste, Italy
[28] University of Turin, Department of Physics, 10125 Turin, Italy
[29] Torino Section of INFN, 10125 Turin, Italy
[30] University of Illinois at Urbana-Champaign, Department of Physics, Urbana, IL 61801-3080, U.S.A.
[31] National Centre for Nuclear Research, 00-681 Warsaw, Poland[v]
[32] University of Warsaw, Faculty of Physics, 02-093 Warsaw, Poland[v]
[33] Warsaw University of Technology, Institute of Radioelectronics, 00-665 Warsaw, Poland[v]
[34] Yamagata University, Yamagata, 992-8510 Japan[t]

[*] Deceased
[a] Also at Instituto Superior Técnico, Universidade de Lisboa, Lisbon, Portugal
[b] Also at Department of Physics, Pusan National University, Busan 609-735, Republic of Korea and at Physics Department, Brookhaven National Laboratory, Upton, NY 11973, U.S.A.
[c] Supported by the DFG cluster of excellence 'Origin and Structure of the Universe' (www.universe-cluster.de)
[d] Also at Chubu University, Kasugai, Aichi, 487-8501 Japan[t]
[e] Also at KEK, 1-1 Oho, Tsukuba, Ibaraki, 305-0801 Japan
[f] Present address: Universität Bonn, Helmholtz-Institut für Strahlen- und Kernphysik, 53115 Bonn, Germany
[g] Also at Moscow Institute of Physics and Technology, Moscow Region, 141700, Russia
[h] Present address: Typesafe AB, Dag Hammarskjölds väg 13, 752 37 Uppsala, Sweden
[i] Supported by Presidential grant NSh - 999.2014.2
[j] Corresponding author
[k] Present address: RWTH Aachen University, III. Physikalisches Institut, 52056 Aachen, Germany
[l] Present address: Uppsala University, Box 516, SE-75120 Uppsala, Sweden
[m] Supported by the DFG Research Training Group Programme 1102 "Physics at Hadron Accelerators"
[n] Supported by the German Bundesministerium für Bildung und Forschung
[o] Supported by EU FP7 (HadronPhysics3, Grant Agreement number 283286)
[p] Supported by Czech Republic MEYS Grant LG13031
[q] Supported by SAIL (CSR), Govt. of India
[r] Supported by CERN-RFBR Grant 12-02-91500
[s] Supported by the Portuguese FCT - Fundação para a Ciência e Tecnologia, COMPETE and QREN, Grants CERN/FP 109323/2009, 116376/2010, 123600/2011 and CERN/FIS-NUC/0017/2015
[t] Supported by the MEXT and the JSPS under the Grants No.18002006, No.20540299 and No.18540281; Daiko Foundation and Yamada Foundation

[u] Supported by the Israel Academy of Sciences and Humanities
[v] Supported by the Polish NCN Grant DEC-2011/01/M/ST2/02350

1 Introduction

The spin structure of the nucleon is one of the major unresolved issues in hadronic physics. While the quark spin contribution to the nucleon spin, denoted as $\Delta\Sigma$, has been measured to be about 30% [1], the gluon spin contribution is still insufficiently constrained after more than two decades of intense study. In the framework of perturbative Quantum Chromodynamics (pQCD), inclusive Deep Inelastic Scattering (DIS) is sensitive to gluon contributions only through higher-order corrections to the cross section. The spin-averaged gluon density $g(x_g)$, where x_g denotes the nucleon momentum fraction carried by gluons, is well constrained by DIS experiments with unpolarised beam and target because of their high statistics and large kinematic coverage. The fewer data from DIS experiments with polarised beam and target, however, can not sufficiently constrain the gluon helicity distribution $\Delta g(x_g)$. This affects directly our knowledge of the contribution of the gluon spin to the spin of the nucleon, known as $\Delta G = \int \Delta g(x_g) dx_g$, and to a lesser extent that of the quarks [2]. In order to better constrain $\Delta g(x_g)$, one has to resort to processes where contributions from gluons appear at leading order, such as hadron production at high transverse momenta or production of open charm in polarised lepton–nucleon [3, 4, 5, 6, 7] or hadron–hadron interactions [8, 9, 10, 11].

The COMPASS collaboration has already investigated asymmetries of hadrons at high transverse momenta p_T, in both the DIS and the quasi-real photoproduction regimes [4, 6, 12]. Here, transverse means transverse with respect to the direction of the virtual photon γ^* that is exchanged in the scattering process. Using a Lund Monte Carlo simulation, these measurements were interpreted on the hadron level, thereby simultaneously extracting the gluon helicity on the parton level. Such an analysis is restricted to leading order (LO) in the strong coupling constant α_s, as presently there exists no next-to-leading order (NLO) Monte Carlo simulation for leptoproduction. Due to the limitation of neglecting gluon contributions at NLO, such results can not be used in recent global fits at NLO of polarised Parton Distribution Functions (PDFs) [13].

In this Letter, we present a new analysis of COMPASS data for single-inclusive hadron quasi-real photoproduction at high p_T [1], which differs from our previous analysis in that all measured hadrons within a given p_T bin are included in the analysis, and not only the hadron(s) with highest p_T. Moreover, the interpretation of the results is based on a collinear pQCD framework that was developed up to NLO [14], the basic concept being the application of the factorisation theorem to calculate the cross section of single-inclusive hadron production. The authors of Ref. [14] discuss the sensitivity of COMPASS data to $\Delta g(x_g)$ in terms of contributions from "direct-photon", $\gamma^* g \to q\bar{q}$ (Photon Gluon Fusion), and from "resolved-photon" subprocesses, qg and gg, where the photon acts as a source of partons. Similarly, they consider direct $\gamma^* q \to qg$ (QCD Compton) as well as resolved qq and gq subprocesses for the background. These contributions to the cross section are represented schematically in Fig. 1. In the framework of collinear fragmentation, photo-absorption on quarks, $\gamma^* q \to q$, is not contributing to high p_T hadron production.

[1] Note that also inclusive quasi-real photoproduction of hadron pairs can be considered [15].

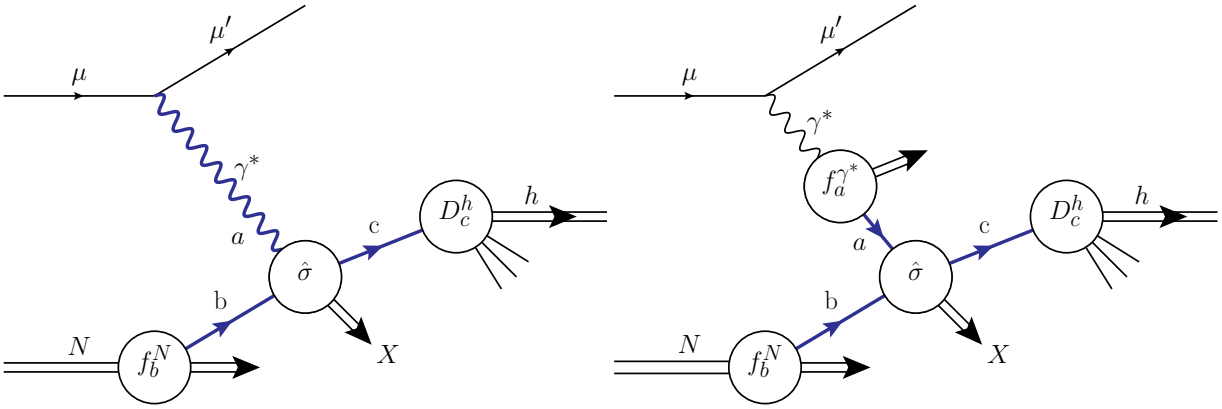

Fig. 1: Contributions to the single-inclusive cross section for quasi-real photoproduction of a hadron h into direct (left) and resolved (right) subprocesses according to Ref. [14]. The internal lines represent the photon $a = \gamma^*$ (left) and partons $\{a,b,c\} = \{q,\bar{q},g\}$. The central blob describes the hard scattering cross section $\hat{\sigma}$. The peripheral blobs describe the non-perturbative objects: parton distributions of the nucleon, f_b^N, and of the photon, $f_a^{\gamma^*}$, and the fragmentation functions of the produced hadron, D_c^h.

In order to gain confidence in the applicability of this pQCD framework to single-hadron production with longitudinally polarised beam and target, an important step is to compare predictions of this model to measurements with beam and target unpolarised, for which the PDFs are well known. While good agreement was found by RHIC experiments on the production of high-p_T hadrons in pp collisions at $\sqrt{s} \simeq 200$ GeV [16, 17], complications arise when hard scattering subprocesses are probed in the "threshold" regime, in which large logarithmic contributions from soft and collinear gluons play a significant role [18]. Such contributions become dominant at the COMPASS centre-of-mass energy of $\sqrt{s} \simeq 18$ GeV. When taken into account by a technique known as "threshold resummation" at next-to-leading logarithm (NLL) [18], the calculations reproduce the COMPASS cross section measurements [19] within theoretical uncertainties.

In this Letter, we analyse the quasi-real photoproduction data collected by COMPASS from 2002 to 2011 on longitudinally polarised deuteron and proton targets. In Sec. 2, we give a brief description of the experimental setup, and details on the data selection can be found in Sec. 3. The procedure for the asymmetry determination is described in Sec. 4. In Sec. 5, we present the corresponding double spin asymmetries for single-inclusive hadron production as a function of their transverse momenta p_T. These asymmetries are compared to calculations that were performed using the code of Ref. [14], which does not include the resummation of threshold logarithms.

2 Experimental Setup

The measurements were performed with the COMPASS setup using positive muons from the M2 beam line of the CERN SPS. A detailed description of the experimental setup can be found in Ref. [20], with updates valid since 2006 described in Ref. [21]. The muon beam had a nominal momentum of 160 GeV/c, except for 2011 where the momentum was 200 GeV/c. On average, its momentum spread was 5 % and its polarisation was $P_b \approx 0.8$. Momentum and trajectory of incident muons were measured by a set of scintillator hodoscopes, scintillating fibre and silicon microstrip detectors. The beam was scattered off a solid state deuterated lithium (^{6}LiD) target from 2002 to 2006 and off an ammonia (NH_3) target in 2007 and 2011, providing longitudinally polarised deuterons and protons, respectively. The target material was placed inside a large aperture superconducting solenoid, and by dynamic nuclear polarisation it was polarised to a value of $P_t \approx 0.5$ for ^{6}LiD and $P_t \approx 0.85$ for NH_3. Until 2004, the target material was contained in two contiguous 60 cm long cells that were oppositely polarised. From

2006 onwards, three contiguous target cells of length 30 cm, 60 cm and 30 cm were used to minimise systematic effects, with the polarisation in the outer cells being opposite to that in the central one. The direction of the target polarisation was regularly flipped by reversing the solenoid field to compensate for acceptance differences between the different target cells. At least once per year, the direction of the polarisation was reversed relative to that of the solenoid field. The dilution factor f, which accounts for the presence of unpolarisable material, amounts to typically 0.4 for the deuterated lithium target and to 0.16 for the ammonia one. It is calculated as the ratio of the cross section on polarisable deuteron or proton to that on all target nuclei, corrected for unpolarised x and y dependent electromagnetic radiative effects [22], where x is the Bjorken scaling variable and y the relative muon energy transfer. No further radiative effects are taken into account. The momenta and angles of scattered muons and produced hadrons were measured in the two-stage open forward spectrometer, where each stage includes a dipole magnet with upstream and downstream tracking detectors.

3 Data Selection

In order to be selected, an event must have an interaction vertex that contains both incoming and scattered muons and at least one hadron candidate track. The measured beam momentum is required to be in a ± 20 GeV interval around the nominal value (± 15 GeV in 2011). In order to equalise the flux through each target cell, the extrapolated beam track is required to pass all target cells. Cuts on the position of the vertex allow the selection of the target cell, in which the scattering occurred. Only events with photon virtuality $Q^2 < 1$ $(\mathrm{GeV}/c)^2$ are accepted. This kinematic region is referred to in the following as quasi-real photoproduction region. In addition, y is required to be within 0.1 and 0.9, where the lower limit removes events that are difficult to reconstruct and the upper limit removes the region where electromagnetic radiative effects are large. These kinematic cuts result in a range of $10^{-5} < x < 0.02$ and a minimum mass squared of the hadronic final state, W^2, of 25 $(\mathrm{GeV}/c^2)^2$. The hadron candidate track must have $p_T > 0.7$ GeV/c. The fraction z of the virtual photon energy carried by the hadron is required to be in the range $0.2 < z < 0.8$, where the lower limit is imposed to suppress the contribution from target remnant hadronisation and the upper limit to reject badly reconstructed hadrons. The angle between the direction of the hadron and that of the virtual photon is restricted to be in the range $10\,\mathrm{mrad} < \theta < 120\,\mathrm{mrad}$, which corresponds to $2.4 > \eta > -0.1$, where η is the pseudo-rapidity in the $\gamma^* N$ centre-of-mass system. After all selections, the final sample consists of 140 million events for the deuteron target and 105 million for the proton target.

4 Asymmetry Calculation

The double-spin asymmetry of the cross sections for single hadron quasi-real photoproduction is defined as $A_{LL} = (\sigma^{\leftrightarrows} - \sigma^{\rightrightarrows})/(\sigma^{\leftrightarrows} + \sigma^{\rightrightarrows}) = \Delta\sigma/\sigma$, where the symbols $\leftrightarrows$ and $\rightrightarrows$ denote anti-parallel and parallel spin directions, respectively, of the incident muon and the target deuteron or proton. This asymmetry is evaluated using the same method as in our previous analyses [6]. The number of hadrons produced in a target cell is related to A_{LL} and to the spin independent cross section $\sigma = \sigma^{\leftrightarrows} + \sigma^{\rightrightarrows}$: $N_i = a_i \phi_i n_i \sigma (1 + f_i P_b P_{t_i} A_{LL})$, where $i = u_1, d_1, u_2, d_2$. A target cell (u or d) with a given direction of the target polarisation (1 or 2) has the acceptance a_i, the incoming muon flux ϕ_i and the number of target nucleons n_i. For the two-cell target, u and d denotes upstream and downstream cell, respectively, while for the three-cell target, u denotes the sum of the outer cells and d the central cell. The asymmetry A_{LL} is extracted from the second order equation that is obtained from the quantity $(N_{u_1} \cdot N_{d_2})/(N_{d_1} \cdot N_{u_2})$. In this relation, fluxes and acceptances cancel, provided that the ratio of acceptances of the two sets of cells is equal for the two orientations of the solenoid field.

In order to minimise statistical uncertainties, all quantities entering the asymmetry are calculated for each hadron using a weight factor $w_i = f_i P_b$ [23]. The muon beam polarisation P_b is obtained from a

parametrisation as a function of the beam momentum. The target polarisation P_{t_i} is not included in the weight w_i as it changes with time and could generate false asymmetries. In order to reduce systematic uncertainties, data are grouped into periods that are close in time and hence have the same detector conditions, and the weighted average over all periods is taken. The asymmetries determined for a given target from data taken in different years were found to be consistent and hence combined. The asymmetries are obtained for both positive and negative unidentified hadrons in bins of p_T in the range 0.7 GeV/c to 4 GeV/c and in bins of η in the range -0.1 to 2.4 in order to facilitate a detailed comparison to theory (see Sec. 5). The data for $p_T < 1.0$ GeV/c are only used to investigate systematic uncertainties as the pQCD framework is commonly applied only for hard scales $\mu^2 \simeq p_T^2 \geq 1.0\,(\mathrm{GeV}/c)^2$, and they are shown greyed out in all the figures where they appear in.

The systematic uncertainties on A_{LL} are calculated as the square root of the sum of squares of multiplicative and additive contributions. The uncertainties on the dilution factor ($\approx 5\%$), the beam ($\approx 5\%$) and the target ($\approx 5\%$) polarisations contribute to a total of $\approx 8\%$ of multiplicative uncertainties, *i.e.* those being proportional to the asymmetry itself. Additive contributions originate from fluctuations of the detector performance, which may lead to false asymmetries. Their possible occurrence is investigated by dividing the data sample into different subsets. Asymmetries calculated with hadrons detected in left and right (top and bottom) parts of the spectrometers are found to be compatible within statistical uncertainties, as well as those for the two relative orientations of the solenoid field and the target spin vectors. No systematic uncertainty is thus attributed to these effects. Possible false asymmetries between data sets having the same polarisation states are also found to be compatible with zero. For each p_T bin, the statistical distribution of the asymmetries calculated by time periods closely follows a normal distribution. The observed deviations from a Gaussian allow us to quantify the level of overall additive systematic uncertainties as a fraction of the statistical ones, which on average amounts to about one half. These additive systematic uncertainties largely dominate over the multiplicative ones.

5 Results and interpretation

The final asymmetries are calculated using all data accumulated with the deuteron target in the years 2002 to 2006 and with the proton target in the years 2007 and 2011. Their p_T-dependence in three rapidity bins spanning the full interval $-0.1 < \eta < 2.4$ ($[-0.1, 0.45]$, $[0.45, 0.9]$, and $[0.9, 2.4]$) is shown in Fig. 2 and Fig. 3 for each target type and hadron charge.

We compare our asymmetries with theoretical calculations at NLO without threshold resummation based on the framework described in Ref. [14] and summarised in the following. Using the code of Ref. [14], the asymmetries are computed in bins of p_T and η as the ratio of polarised to unpolarised hadron cross sections, where a cross section is a convolution of the "muon–parton distribution function" f_a^μ, the nucleon PDFs f_b^N, the perturbative partonic cross sections $\hat{\sigma}_{a+b\to c+X}$, and the fragmentation functions (FF) D_c^h:

$$A_{LL}(p_T,\eta) = \frac{\mathrm{d}\Delta\sigma^h}{\mathrm{d}\sigma^h}(p_T,\eta) = \frac{\sum_{a,b,c} \Delta f_a^\mu \otimes \Delta f_b^N \otimes \mathrm{d}\Delta\hat{\sigma}_{a+b\to c+X} \otimes D_c^h}{\sum_{a,b,c} f_a^\mu \otimes f_b^N \otimes \mathrm{d}\hat{\sigma}_{a+b\to c+X} \otimes D_c^h} \,. \tag{1}$$

Here and below, spin-dependent quantities are denoted by the symbol Δ and will be referred to as polarised ones in the rest of the Letter (spin-independent ones as unpolarised). The processes involved in Eq. 1 can be classified into "direct" ones that are initiated by a quasi-real photon and "resolved" ones that are initiated by its fluctuation into partons. This classification is denoted by the subscript a (see Fig. 1). For direct processes, subscript a refers to γ^*, and $(\Delta)f_{\gamma^*}^\mu$ is the probability for a muon to emit a quasi-real photon. For resolved processes, subscript a refers to q, $\bar{q}$ or g, and $(\Delta)f_a^\mu$ is the convolution of this probability with a non-perturbative parton distribution of the photon, $(\Delta)f_a^{\gamma^*}$. The polarised version

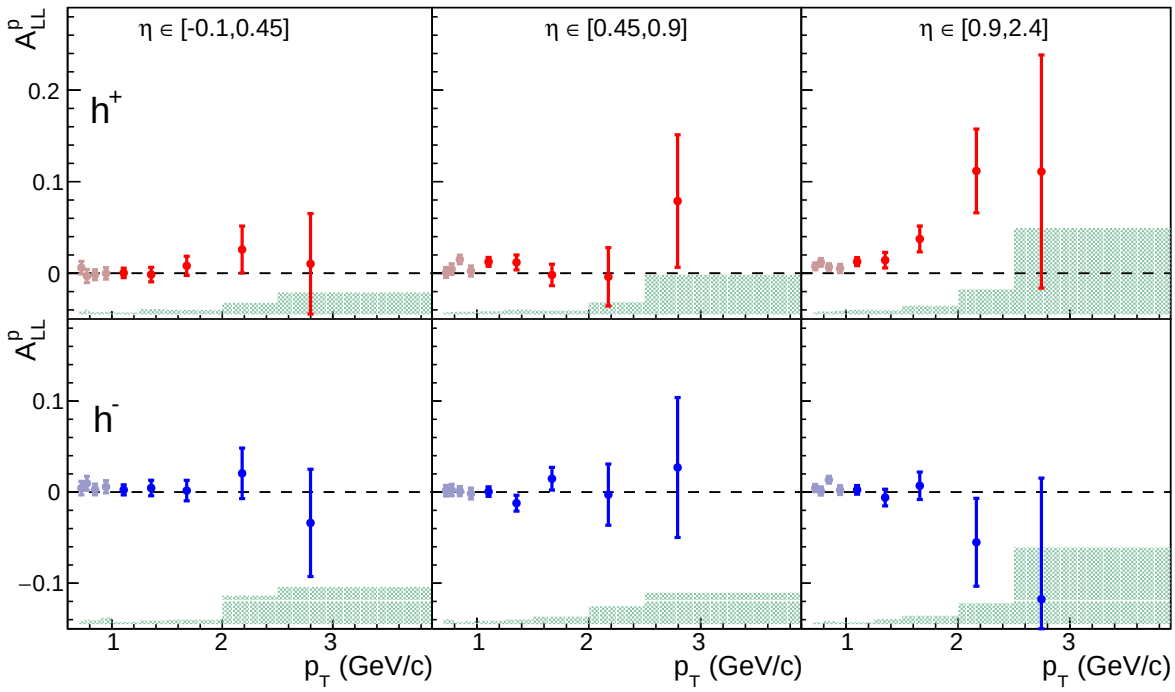

Fig. 2: The asymmetry A_{LL} as a function of p_T for charged hadron quasi-real photoproduction on the proton for three rapidity bins. The bands at the bottom indicate the systematic uncertainties, which are dominated by time dependent fluctuations (see Sec. 4.) Top: positive hadron production; bottom: negative hadron production.

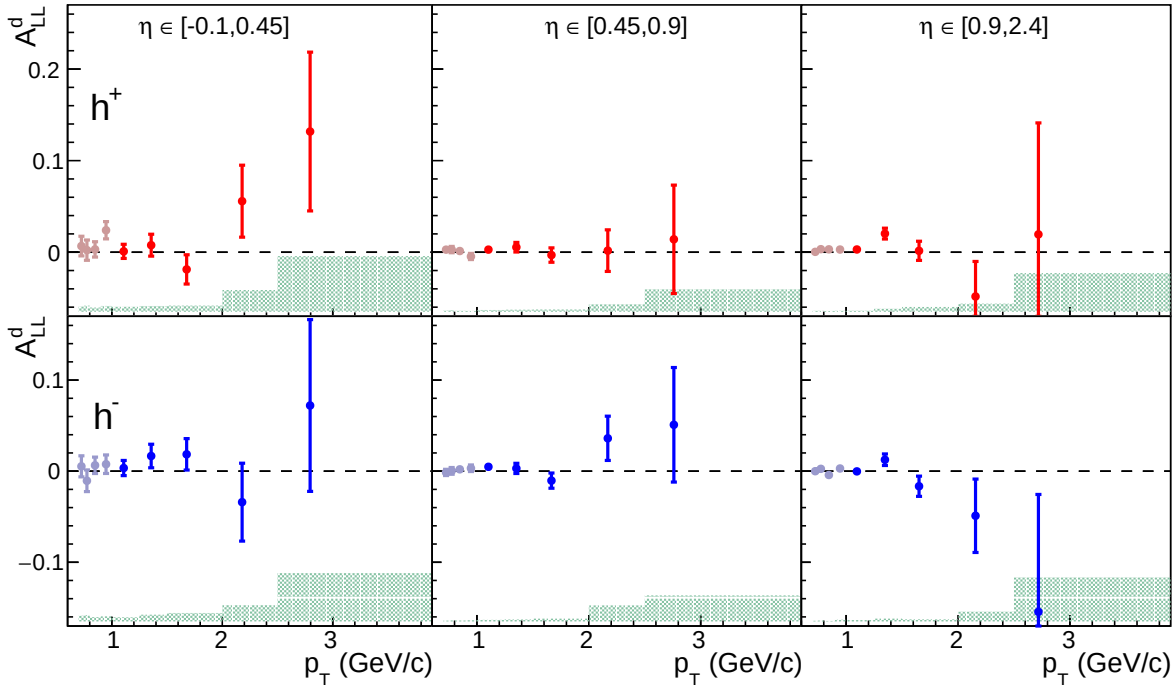

Fig. 3: Same as Fig. 2, but for the deuteron.

of the latter is not known experimentally and hence taken to range between the positive and negative magnitude of the unpolarised one. This induces a small uncertainty in the theoretical calculations.

The values of the asymmetries are computed here using the following input distributions: the unpolarised parton distributions of the photon $f_a^{\gamma^*}$ from GRS[24], the unpolarised nucleon PDFs f_b^N from CTEQ65[25], the three polarised PDF sets from GRSV[26] as in Ref. [14] (the "standard" set and the two sets for "maximum" [$\Delta g(x) = g(x)$] and "minimum" [$\Delta g(x) = -g(x)$] gluon distribution functions at input scale), as well as the most recent polarised PDF set DSSV14 from Ref. [13]. For the polarised PDF sets used, the integration over the range $0.05 < x_g < 0.2$, which is characteristic for the kinematic coverage of COMPASS in the gluon momentum fraction, yields the following "truncated" values of ΔG at a scale of 3 $(\mathrm{GeV}/c)^2$: $\Delta G_{GRSV_{min}} \approx -0.6$, $\Delta G_{DSSV14} \approx 0.1$, $\Delta G_{GRSV_{std}} \approx 0.2$, $\Delta G_{GRSV_{max}} \approx 0.7$. The other inputs that we changed with respect to Ref. [14] are the fragmentation functions D_c^h, for which we use the most recent parton-to-pion fragmentation set of Ref. [27], which best fits the recent COMPASS pion multiplicities [28]. We checked, as it was done in Ref. [14], that asymmetries for hadron and pion production are almost indistinguishable, so that it is safe to compare our experimental data to theoretical asymmetries computed with a parton-to-pion FF set. The fractions of the total unpolarised (respectively polarised) cross section for the various individual subprocesses are shown in Fig. 4 as a function of p_T. Although the unpolarised cross sections for processes involving gluons from the nucleon are not the dominant ones, the polarised cross section for the γg subprocess is large in magnitude for hadron production at high p_T, which makes the study of such asymmetries relevant in the COMPASS kinematic region.

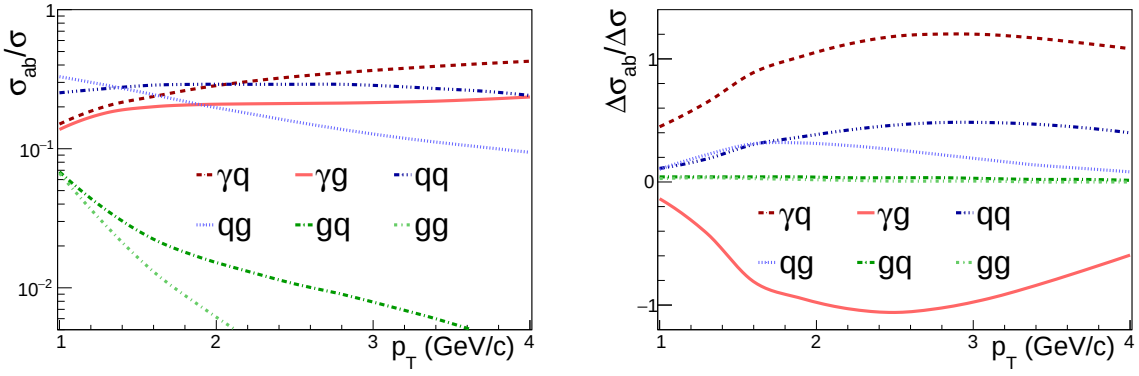

Fig. 4: Contributions of the six subprocesses $a+b \to c+X$ described in Sec. 1 to the full NLO unpolarised (left) and polarised (right) photoproduction cross sections for a deuteron target. The polarised cross sections are computed using the polarised PDF set of Ref. [13].

The computations of $A_{LL}(p_T)$ are performed at COMPASS kinematics using the same cuts as in the present data analysis, *i.e.*, $p_T > 1\,\mathrm{GeV}/c$, $Q^2 < 1\,(\mathrm{GeV}/c)^2$, $0.1 < y < 0.9$, $0.2 < z < 0.8$. For consistency, we verified that when using the same inputs as in Ref. [14], we reproduce the asymmetry calculated there. The computations are done separately for the production of positive and negative hadrons, and for three distinct bins in η: $[-0.1, 0.45]$, $[0.45, 0.9]$, and $[0.9, 2.4]$. The results of these computations are compared to the experimental asymmetries in Fig. 5 and Fig. 6.

The data are seen to be consistent with the NLO calculations of Ref. [14] using the most recent polarised PDF [13] and FF [27] sets, except for positive hadron production from the proton in the rapidity range $-0.1 < \eta < 0.9$. Our data are also compared in Fig. 5 and Fig. 6 to calculations using earlier GRSV polarised PDFs [26] to give an impression of their sensitivity to ΔG, which seems enhanced at higher values of η. A possible reason for the discrepancy seen at low η in positive hadron production from the proton may be that the model calculations had to be done without threshold resummation at NLL, as the formalism for the polarised case is not yet fully available. However, contrary to the unpolarised case

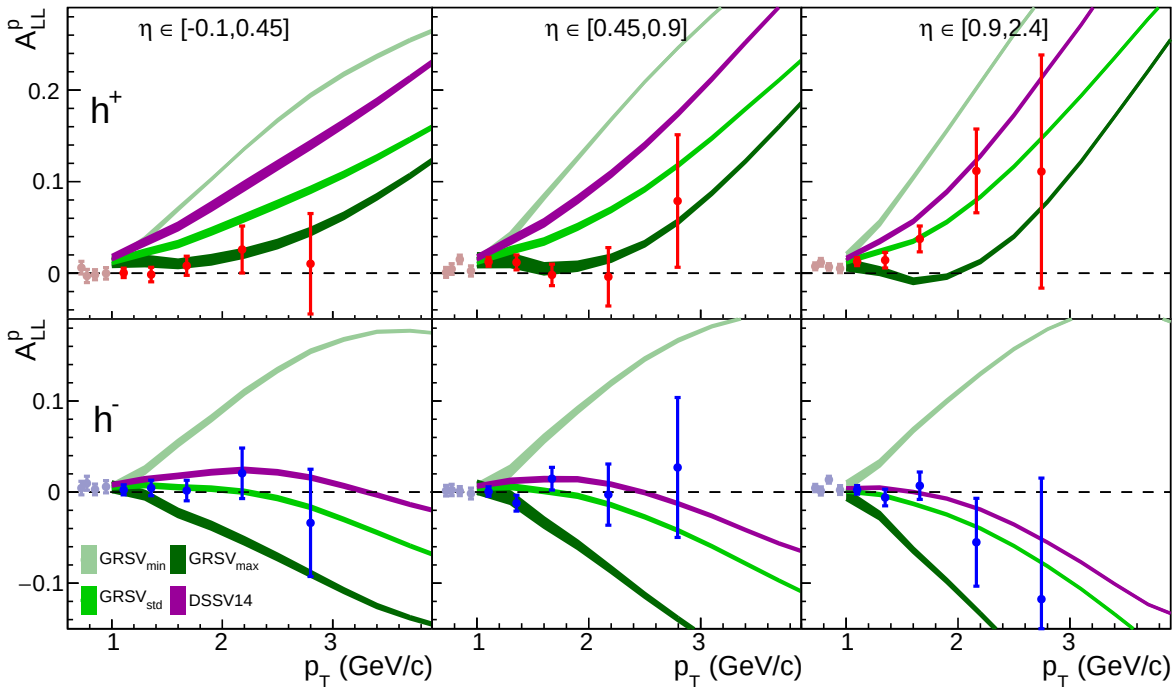

Fig. 5: COMPASS asymmetries A_{LL} for a proton target as a function of p_T and in three rapidity bins, compared to NLO calculations based on Ref. [14] for different choices for the polarised PDFs (see text). Only statistical uncertainties are shown. Error bands on the theory curves represent the uncertainties due to the polarised parton distribution of the photon. Top: positive hadron production; bottom: negative hadron production.

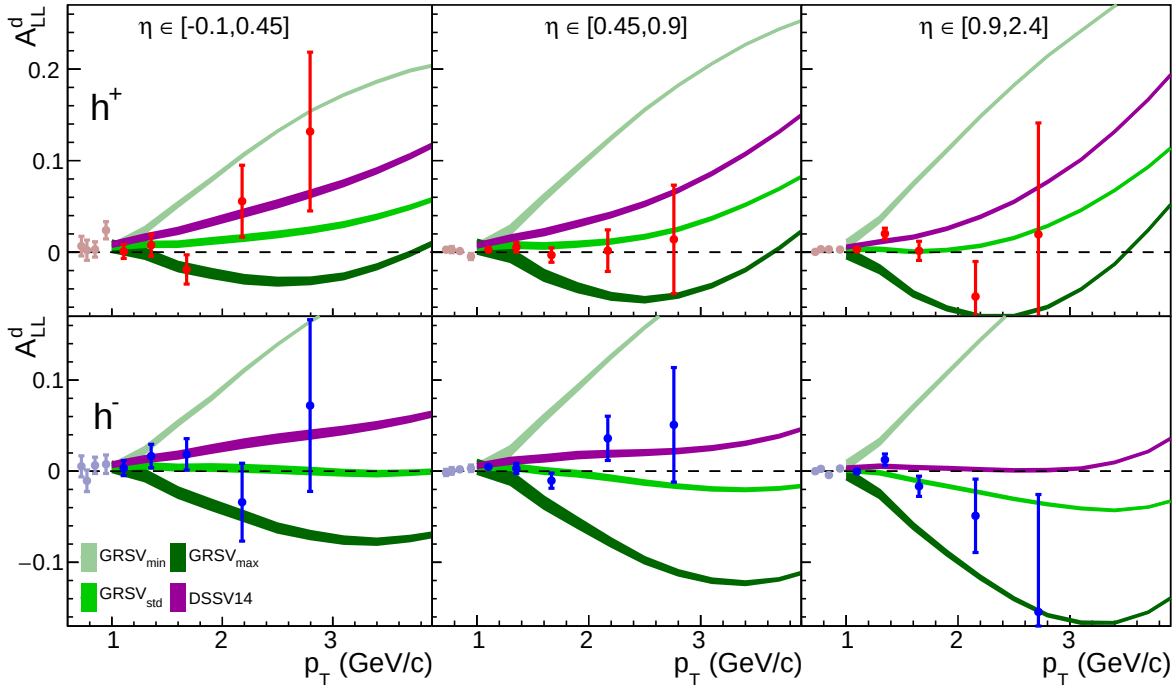

Fig. 6: Same as Fig. 5, but for a deuteron target.

where data can only be described by pQCD if threshold resummation is included [18][2], spin asymmetries are expected to be less affected [29]. A first estimation of the impact of threshold resummation on our double spin asymmetries including so far only the direct processes [30] indicates a substantial dilution of the asymmetries, which may explain part of the discrepancy between experiment and theory for positive hadron production on the proton at low values of η.

6 Summary

In summary, we have presented in this Letter a new analysis of COMPASS data on polarised single-inclusive hadron quasi-real photoproduction, which in principle is well suited for an extraction of the gluon polarisation ΔG in the framework of collinear pQCD. Results for the longitudinal spin asymmetry $A_{LL}(p_T)$ on polarised protons and deuterons are given separately for positively and negatively charged hadrons, and in three rapidity bins. They are compared to theoretical calculations at NLO without threshold resummation and overall agreement is found with the calculations based on earlier GRSV$_{std}$ and recent DSSV14 polarised PDF sets, and using the most recent FF set. Nevertheless, calculations including full threshold resummation at NLL are needed before a meaningful result on ΔG can be extracted quantitatively from our data.

Acknowledgements

We thank Werner Vogelsang and Marco Stratmann for many useful discussions and for providing us the codes for the NLO pQCD calculation. We gratefully acknowledge the support of the CERN management and staff and the skill and effort of the technicians of our collaborating institutes. This work was made possible by the financial support of our funding agencies.

References

[1] C.A. Aidala, S.D. Bass, D. Hasch and G.K. Mallot, Rev. Mod. Phys. 85 (2013) 655.
[2] COMPASS Collaboration, C. Adolph et al., submitted to Phys. Lett. B, arXiv:1503.08935.
[3] SMC Collaboration, B. Adeva et al., Phys. Rev. D 70 (2004) 012002.
[4] COMPASS Collaboration, E.S. Ageev et al., Phys. Lett. B 633 (2006) 25.
[5] HERMES Collaboration, A. Airapetian et al., JHEP 08 (2010) 130.
[6] COMPASS Collaboration, C. Adolph et al., Phys. Lett. B 718 (2013) 922.
[7] COMPASS Collaboration, C. Adolph et al., Phys. Rev. D 87 (2013) 052018.
[8] STAR Collaboration, L. Adamczyk et al., Phys. Rev. D 89 (2014) 012001.
[9] PHENIX Collaboration, A. Adare et al., Phys. Rev. D 90 (2014) 012007.
[10] PHENIX Collaboration, A. Adare et al., Phys. Rev. D 84 (2011) 012006.
[11] STAR Collaboration, L. Adamczyk et al., Phys. Rev. Lett. 115 (2015) 092002.
[12] COMPASS Collaboration, M. Stolarski, A new LO extraction of gluon polarisation from COMPASS DIS data, 22nd International Workshop on Deep-Inelastic Scattering and Related Subjects, Warsaw, Poland, April 28 – May 2 2014, pp. 211.
[13] D. de Florian, R. Sassot, M. Stratmann and W. Vogelsang, Phys. Rev. Lett. 113 (2014) 012001.
[14] B. Jäger, M. Stratmann and W. Vogelsang, Eur. Phys. J. C 44 (2005) 533.
[15] C. Hendlmeier, M. Stratmann and A. Schäfer, Eur. Phys. J. C 55 (2008) 597.
[16] PHENIX Collaboration, A. Adare et al., Phys. Rev. D 76 (2007) 051106.

[2] In Ref. [19], the validity of the formalism [18] was verified in the full η and p_T range covered by COMPASS kinematics. This statement does not suffer from slightly larger y and Q^2 cuts used in the present analysis to enhance statistics, as we checked that the asymmetries obtained for the two sets of cuts are compatible within statistical uncertainties.

[17] STAR Collaboration, B.I. Abelev et al., Phys. Rev. D 80 (2009) 111108.
[18] D. de Florian, M. Pfeuffer, A. Schäfer and W. Vogelsang, Phys. Rev. D 88 (2013) 014024.
[19] COMPASS Collaboration, C. Adolph et al., Phys. Rev. D 88 (2013) 091101.
[20] COMPASS Collaboration, P. Abbon et al., Nucl. Instr. Meth. A 577 (2007) 455.
[21] COMPASS Collaboration, P. Abbon et al., Nucl. Instr. Meth. A 779 (2015) 69.
[22] COMPASS Collaboration, V. Alexakhin et al., Phys. Lett. B 647 (2007) 330.
[23] SMC Collaboration, D. Adams et al., Phys. Rev. D 56 (1997) 5330.
[24] M. Glück, E. Reya and I. Schienbein, Phys. Rev. D 60 (1999) 054019.
[25] J. Pumplin et al., JHEP 07 (2002) 012.
[26] M. Glück, E. Reya, M. Stratmann and W. Vogelsang, Phys. Rev. D 63 (2001) 094005.
[27] D. de Florian, R. Sassot, M. Epele, R.J. Hernández-Pinto and M. Stratmann, Phys. Rev. D 91 (2015) 014035.
[28] COMPASS Collaboration, N. Makke, Fragmentation Functions measurement at COMPASS, 21st International Workshop on Deep-Inelastic Scattering and Related Subjects, Marseille, France, Apr 22-26 2013, pp.202; arXiv:1307.3407.
[29] D.P. Anderle, F. Ringer and W. Vogelsang, Phys. Rev. D 87 (2013) 094021.
[30] C. Uebler, A. Schäfer and W. Vogelsang, arXiv:1510.01058.